AIRPORT PAVEMENT DISTRESS IMAGE CLASSIFICATION USING MOMENT INVARIANT NEURAL NETWORK

Chun-Jung Hsu, Chi-Farn Chen, Chau Lee, Shu-Meng Huang

Center for Space and Remote Sensing Research
National Central University,
Chung-Li, TAIWAN
Tel: (886)-3-4227151-7698, Fax: (886)-3-4254908
E-mail: hsujoker@csrsr.ncu.edu.tw

KEY WORDS: Airport Pavement Distress, Moment Invariant, Neural Network

ABSTRACT: In this paper we present moment invariant and neural network to classify airport pavement distress images. The moment invariant has been extracting images feature that published two-dimensional pattern recognition application method in 1962. The image pattern can be reduced to number of values such that they are description of the translation, scale, and rotation of an object in the image. In this paper we investigate the technique of moment invariant for the crack image of feature extraction. Then the neural network that we use back-propagation learning in its training, classifying these feature, and attempts to produce the desired output. The real crack images are always not pure distress features. However, the back-propagation neural network may be used to provide fitness against noise. The results indicate that using moment invariant and neural network to provide accurate classification processing in various types of airport pavement distress.

1. INTRODUCTION

Nothing is more important than emphasizing the importance of Aviation Safety due to the blooming of the mass transportation. Therefore, the maintenance for runway, taxiway and apron has become essential parts of Aviation Safety. Presently, since the inspection methods of airport pavement are mostly by means of optic investigation, which is neither effective nor rapid. Moreover, the less experienced, moody or fatigued investigators have sometimes led to erroneous or bungling estimate of pavement distress. Furthermore, the frequency of flights, such as ones in the Sung-Shan Airport, takes off or land approximately every five minutes has caused the difficulties of investigation during the daytime. Although the investigation must shift to the nighttime while the airport is closed, the investigation conclusions were still unreliable because of the ray source of synthetic illuminant.

In spite of that, the problems can be solved through technology, such as GPS, GIS and image capture to grab the related information of pavement distress (Lee, 2001). We progressively apply the technique of image identification: Firstly capture a true color image, secondly transfer and process image into gray scale image. After being extracted from the gray scale image and removed the non-crack image, the image has become binary image. Afterwards, we administer the moment invariants to describe the image characterization. Still, these characterizations have to be normalized to be the input values of neural network. Subsequent to learning and training in neural network, it is able to identify types of pavement distress and degrees of their severity.

In this paper we take the Sung-Shan Airport as an example to investigate the pavement distress images. We use image processing to get binary images and moment invariant to get values of characterization. As a result, we have taken a great step on introducing the integration of back-propagation neural network and normalized value of moment invariant to identify several types of pavement distress and their maintenance methods. It is also an essential consult to maintenance technical, analyses and discussion issues of progressive pavement distress in the near future.

2. METHODOLOGY

2.1 Image Processing

First of all, we let the true color image transfer into gray scale image, for concrete pavement cracks and distress are mostly with dark color. Hence, we use threshold to separate the gray scale values and to extract the distress parts, progressively develop the image enhancement and image filtering of the binary images to filter little noise and to produce the extraction resources of image characterization.

2.2 Moment Invariant

Hu dedicated the Moment Invariant[1] in 1962 regarding the Algebraic Images theory, evolved the algebraic values of two-dimensional images obtained by non-liner combination equation to describe the geometric characteristics (P. Raveendran, 1991). To translate, scale and rotate images, the specified values can evolve invariant to describe the geographic characterization. Therefore, it broadly has been made use to identify aircraft fighters, word fonts and other related images these years, while the computer technology commenced to bloom.
The basic definition for moment invariant (Lee, 1999) is as follows:

$$m_{pq} = \int_{-\infty}^{\infty}\int_{-\infty}^{\infty} x^p y^q f(x,y)dxdy \quad (1)$$

The x, y represents for coordinate of x direction and y direction. $f(x, y)$ means this coordinate position correspond to the value of gray degreed, then the above definition progressively change into central moments, the formula is as follows:

$$m_{pq} = \int_{-\infty}^{\infty}\int_{-\infty}^{\infty} (x-\bar{x})^p (y-\bar{y})^q f(x,y)dxdy \quad (2)$$

$$\bar{x} = \frac{m_{10}}{m_{00}} \qquad \bar{y} = \frac{m_{01}}{m_{00}}$$

The above formula is per continue function, and is a scattered function; therefore, we have to change the central moment into scattered function as follows:

$$m_{pq} = \sum_x \sum_y (x-\bar{x})^p (y-\bar{y})^q f(x,y) \quad (3)$$

To be the resource of non-liner function combination, the central moments of scattered function has to be standardized; the standardized formula is as below:

$$g = \frac{p+q}{2}+1, \quad p+q = 2,3,4..... \quad (4)$$
$$h_{pq} = \frac{m_{pq}}{m_{00}^g}$$

After being standardized, the central moment can be progressed to the following formula of non-liner scattered Combination for image characteristic values (Chou, 1994):

Hu Moment Invariants:

The seven moments up to three orders are shown:

$$\begin{aligned}
HM_1 &= h_{20} + h_{02} \\
HM_2 &= (h_{20} - h_{02})^2 + 4h_{11}{}^2 \\
HM_3 &= (h_{30} - 3h_{12})^2 + (3h_{21} - h_{03})^2 \\
HM_4 &= (h_{30} + h_{12})^2 + (3h_{21} + h_{03})^2 \\
HM_5 &= (h_{30} - 3h_{12})(h_{30} + h_{12})\left[(h_{30} + h_{12})^2 - 3(h_{21} + h_{03})^2\right] \\
&\quad + (3h_{21} - h_{03})(h_{21} + h_{03})\left[3(h_{30} + h_{12})^2 - (h_{21} + h_{03})^2\right] \\
HM_6 &= (h_{20} - h_{02})\left[(h_{30} + h_{12})^2 - (h_{21} + h_{03})^2\right] \\
&\quad + 4h_{11}(h_{30} + h_{12})(h_{21} + h_{03}) \\
HM_7 &= (3h_{21} - h_{30})(h_{30} + h_{12})\left[(h_{30} + h_{12})^2 - 3(h_{21} + h_{03})^2\right] \\
&\quad + (3h_{21} - h_{30})(h_{21} + h_{03})\left[3(h_{30} + h_{12})^2 - (h_{21} + h_{03})^2\right] \quad (5)
\end{aligned}$$

[1] His approach is based on the work of the nineteenth century mathematicians Boole, Cayley and Sylvester, the theory of algebraic form.

Bamieh Moment Invariants

The Ba mieh Moment Invariants can be expressed by using central moments as shown:

$$
\begin{aligned}
BM_1 &= h_{02}h_{20} - h_{11}^{\ 2} \\
BM_2 &= (h_{03}h_{30} - h_{21}h_{12})^2 - 4(h_{03}h_{12} - h_{21}^{\ 2})(h_{21}h_{30} - h_{12}^{\ 2}) \\
BM_3 &= h_{40}h_{04} - 4h_{31}h_{13} + 3h_{22}^{\ 2} \\
BM_4 &= h_{40}h_{22}h_{04} - 2h_{31}h_{22}h_{13} - h_{40}h_{13}^{\ 2} - h_{04}h_{31}^{\ 2} - h_{22}^{\ 3}
\end{aligned} \tag{6}
$$

Zernike Moment Invariants

The Zernike Moment expressed in terms of usual central moments are shown:

$$
\begin{aligned}
ZM_1 &= \frac{3}{p}[2(h_{20} + h_{02}) - 1] \\
ZM_2 &= \frac{9}{p^2}[(h_{20} - h_{02})^2 + 4h_{11}^{\ 2}] \\
ZM_3 &= \frac{16}{p^2}[(h_{03} - 3h_{21})^2 + (h_{30} - 3h_{12})^2] \\
ZM_4 &= \frac{144}{p^2}[(h_{03} + h_{21})^2 + (h_{30} + h_{12})^2] \\
ZM_5 &= \frac{13824}{p^4}\{(h_{03} - 3h_{21})(h_{03} + h_{21})[(h_{03} + h_{21})^2 - 3(h_{30} + h_{12})^2] \\
&\quad - (h_{30} - 3h_{12})(h_{30} + h_{12})[(h_{30} + h_{12})^2 - 3(h_{03} + h_{21})^2]\} \\
ZM_6 &= \frac{864}{p^3}\{(h_{02} - h_{20})[(h_{30} + h_{12})^2 - (h_{03} + h_{21})^2] + 4h_{11}(h_{03} + h_{21})(h_{30} + h_{12})\}
\end{aligned} \tag{7}
$$

To get specific values, we put Binary images into the above formulas. Because the range of values is large, the specific values have to be normalized to reduce the ranges for scope of value and to provide input training and learning samples in neural network. the process is as below:

1. Make 10 as logarithmic base (i.e. log 10), to reduce the value ranges and to avert from ultra scopes.
2. Sum up individual invariant values divide root mean square of invariant, shown as below:

$$
m_i' = \frac{m_i}{\sqrt{\sum_i^n m_i^2}} \tag{8}
$$

2.3 Back-Propagation Neural Network

The primary principle for back-propagation neural network is by using the idea of the gradient steepest descent method to minimize the error function. It also belongs to the supervised learning network, which is applied to diagnosis, prediction, etc. (Lin, 1993). The framework of network is shown as Figure 1:

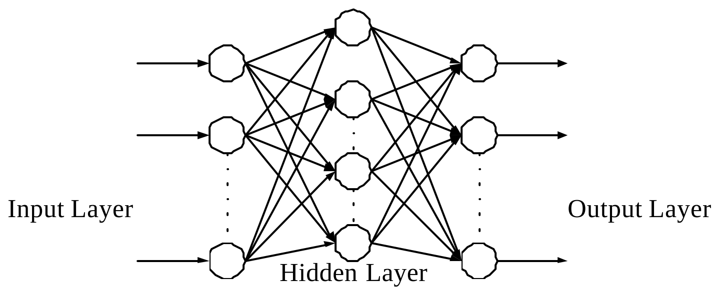

Figure 1, the framework of back-propagation neural network

Except for the input layer applies the liner transformation function (i.e. $f(x) = x$) and hidden layer applies the non-liner transformation function, most applications apply the sigmoid function, shown as below:

$$f(x) = \frac{1}{1+e^{-x}} \tag{8}$$

When a variable is similar to plus infinity, the function value is similar to 1; on the other hand, while a variable is similar to minus infinity, the function of values is similar to zero. In another words, the value of range function is between one and zero.
We have to dive samples into two types during learning recurrence: learning samples and testing samples. In the stage of learning recurrence, put the test samples to network to test if the error degrees in network are convergent and to inspect whether the training errors and test errors are in consistence. That is to say, to inspect if the training samples are able to be representative samples. In addition, during the process of inspection, it is necessary to observe if the testing samples are objective.
There are two types of error functions:
1. The Error of RMS equation:

$$RMS = \sqrt{\frac{\sum_{P}^{M}\sum_{j}^{N}\left(T_j^P - Y_j^P\right)^2}{M \cdot N}} \tag{9}$$

T_j^P : target output values of output unit no. j in example no. P

Y_j^P : inference output values of output unit no. j in example no. P

M: number of examples

N: numbers of output layers processing units

2. Total rate of errors:
Total rate of errors = sum of error classification examples / sum of examples
Total rate of errors is more deliberate regarding that there is only one correct classification question for each example.
With respect to our research of using Error Function, the Total Rate of Errors can assist us to understand the convergence degree of Error Square Root. Consequently, we will recognize if Learning Samples are consistent with Test Samples. Furthermore, the Total Rate of Errors can help us determine the ability of learning distinguish in Neural Networks,

3. RESULTS

We seize the Sung-San Airport as the research district to actually shoot for and administer pavement distress images. Through normalization, we got 17 specific values of moments invariant, as well as the important attribution for the airport, etc. to be the input layer nods for neural network.
There are four kinds of pavement distress for an output layer: vertical cracks, horizontal cracks, netted cracks and cavities; also three types of maintenance degrees: no needs, trivial repairs and urgent repairs. Besides, there are 13 nods for a hidden Layer, 80 training samples and 40 testing samples. The totally frequency is 1,200 cycles of practicing learning. After the practicing of learning and training, we got the error rate of convergence conditions as shown in Figure 2:

Figure 2, Error rate of convergence conditions

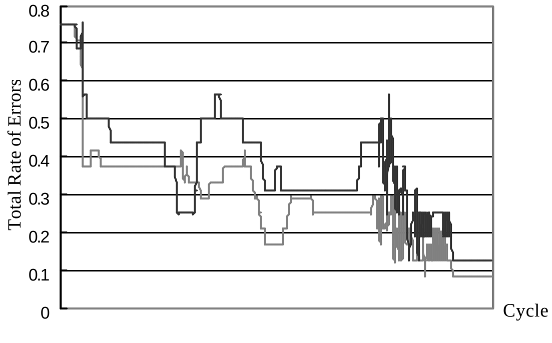

The above graphic explains that error convergence curves for both training and testing samples are similar and conformable. Because of the samples are in sufficient quantity and with less conflicts, they are accordingly delegable and with representation. In addition, the successful rate for the result of recalls from the back-propagation neural network is 85%, which can be the methods of distinguishing pavement distress and the maintenance techniques.

4. CONCLUSION

This paper is to administer information of location attribution and images of pavement distress through the theories of moment invariant and back-propagation neural network. The excellent outcomes for identification of the types of distress and degrees of maintenance have assisted to be the sources of airport maintenance and accelerate the future researches such as maintenance techniques and their methods.

5. REFERENCE

Chou, JaChing, Wende A. O'Neill, H.D. Cheng, 1994. Pavement Distress Classification Using Neural Networks. Systems, Mans, and Cybernetics, Humans Information and Technology, 1994 IEEE International Conference on Vol. 1, pp.397-401.

Kulkarni, A. D., Al. C. Yap, P. Byars, 1990. Neural Networks for Invariant Object Recognition. Applied Computing, Proceedings of the 1990 Symposium on, pp.28-32.

Lee, Chau, C.F. Chen, Shu-Meng Huang, Chun-Jung Hsu, 2001. An Automated Airport Pavement Image Survey System. AISA GIS 2001 Conference.

Lee, Jen-Dao, 1999. Characters comply to images Commence to compliance in application study. National Central University Civil Engineering Department, master essay.

Lin, Joo, 1993. Application and Practice of Neural Networks Model., edited by Yi-Cheng Yeh, Taipei, pp4-1~51, pp21-1~34.

McAulay, A., A. Coker, K. Sauhan, 1991. Effect of Noise in Moment Invariant Neural Network Aircraft Classification", Aerospace and Electronics Conference, Proceedings of the IEEE 1991 National, Vol. 2, pp.743-749.

Raveendran, P., Sigeru Omatu, Ong Seng Huat, 1991. Moment Invariant Features used as Inputs to a Neural Network to Recognize Numerals. TENCON'91 IEEE Region 10 International Conference on EC3-Energy, Computer, Communication and Control Systems Vol. 1, pp.141-143.